Reversible Supra-Folding of User-Programmed Functional DNA Nanostructures on Fuzzy Cationic Substrates

Koyomi Nakazawa, Farah El Fakih, Vincent Jallet, Caroline Rossi-Gendron, Marina Mariconti, Léa Chocron, Mafumi Hishida, Kazuya Saito, Mathieu Morel, Sergii Rudiuk, et al.

Reversible supra-folding of user-programmed functional DNA nanostructures on fuzzy cationic substrates

Koyomi Nakazawa[a,b], Farah El Fakih[a], Vincent Jallet[a], Caroline Rossi–Gendron[a], Marina Mariconti[a], Léa Chocron[a], Mafumi Hishida[b], Kazuya Saito[b], Mathieu Morel[a], Sergii Rudiuk*[a], Damien Baigl*[a]

Abstract: Programmable DNA base pairing is a powerful way to build user-defined nanostructured assemblies, such as DNA origamis and DNA nanogrids. Although two-dimensional (2D) origamis of virtually any desired shape can now be quickly and easily produced, attaining further levels of organization, actuation or dynamics is still a desired challenge. Here we report that, upon adsorption on a soft cationic substrate prepared by layer-by-layer deposition of polyelectrolytes, both 2D origamis and DNA nanogrids undergo a rapid higher-order transition of folding into three-dimensional (3D) compact structures (origamis) or well-defined µm-long ribbons (nanogrids), a process we refer to as supra-folding. We show that the supra-folding mechanism is mainly of electrostatic nature through on-surface inter-polyelectrolyte complexation, thus requiring enough fuzziness of the substrate to allow 3D reconfiguration instead of conventional flat adsorption. Interestingly the electrostatic nature of this actuation makes it reversible: once supra-folded, origamis can be switched back on the surface into their 2D original shape through addition of heparin, a highly charged anionic polyelectrolyte known as an efficient competitor of DNA-polyelectrolyte complexation. Orthogonal to DNA base-pairing principles, this reversible structural reconfiguration is also versatile; we show in particular that i) it is compatible with various origami shapes, ii) it perfectly preserves fine structural details as well as site-specific functionality, and iii) it can be applied to dynamically address the spatial distribution of origami-tethered proteins.

DNA preserves and transfers genetic information due to the complementarity between two polynucleotide strands assembled according to Watson-Crick base-pairing.[1] The strong specificity of hydrogen bonding within the base-pairs is a unique property of DNA which has enabled wide applications not only in biomedical research but also in materials science, with the development of molecular computers and programmed self-assembly systems.[2–4] For instance, the formation of well-organized microscale objects such as nanorobots, biomimetic systems and programmed colloidal systems[3,5] have been achieved by using precisely designed sequences of DNA oligonucleotides. One widely used approach consists in folding a long single-stranded circular DNA template chain into intended nanostructures called DNA origamis, by specific hybridization with a large number of short single-stranded DNA oligonucleotides (staples).[6] This technique enables the realization of DNA nanostructures of virtually any desired shape[7–10] with high site accuracy and yield.[11] The conventional method leads however to the formation of two-dimensional (2D) and intrinsically static objects. To achieve nanosystems with advanced functionalities, efforts have been devoted to increase the structural complexity of DNA origamis, especially to build three-dimensional (3D) nano-objects.[8,9,12–15] Those could be obtained using proper sequence designs but require rather long formation time to ensure flawless assembly. Another challenge was to render DNA origamis dynamic with the realization of stimulus-responsive behavior or on-demand morphological change capability.[15–17] This was successfully achieved by mostly following DNA base pairing principles. Additionally, dynamic responses could be obtained through the use of strand-displacement strategies[18] that necessitate specific configurations where the replacement of one or several oligonucleotides can dramatically affect the overall DNA origami shape.[16,17] Other approaches for external actuation of DNA origamis using stimuli such as light, pH, ionic concentration and magnetic field have also been demonstrated,[16,17] but usually requiring specific modifications of DNA to make it stimulus-responsive. It is thus important to devise new approaches for actuation of DNA origamis and other user-programmed nanostructures, with the requirement to be orthogonal to DNA base-pairing and without need of DNA covalent modification. This was investigated in a few cases, for instance by using salts,[19] DNA intercalator[20], supported lipid bilayer[21,22] and crowding effect with poly-(ethylene glycol)[23]. Electrostatic interaction is a key-parameter[24] that has also been applied for formation of superlattice and new structures by addition of charged objects[25,26] as well as for actuation by simply applying voltage.[27] In the present study, we first investigated the behavior of 2D DNA origamis onto soft cationic substrates composed of polymers and discovered a surprising behavior. Although origamis were adsorbing flat on cationic polymeric monolayers, they underwent an additional folding step on themselves, referred to as supra-folding, when they adsorbed on positive substrates prepared by layer-by-layer polyelectrolyte deposition. This led to the formation of a new kind of self-folded 3D nanostructures. Notably, this supra-folding was found to be reversible, as the structures were efficiently unfolded back into their native 2D shapes upon addition of a competitive anionic polyelectrolyte. We investigated the role of the substrate in this phenomenon as well as the applicability of this actuation method to structurally reconfigure various DNA nanostructures including origamis of different shapes and functions as well as DNA nanogrids.

[a] Dr. K. Nakazawa, Ms F. El Fakih, Dr. V. Jallet, Dr. C. Rossi–Gendron, Ms M. Mariconti, Ms. Léa Chocron, Dr. M. Morel, Dr. S. Rudiuk, Prof. Dr. D. Baigl
PASTEUR, Department of Chemistry, Ecole Normale Supérieure, PSL University, Sorbonne Université, CNRS 75005 Paris (France)
E-mail: damien.baigl@ens.psl.eu, sergii.rudiuk@ens.psl.eu

[b] Dr. K. Nakazawa, Dr. M. Hishida, Prof. K. Saito
Department of Chemistry, University of Tsukuba, Tsukuba, Ibaraki 305-8571, Japan

Supporting information for this article is given via a link at the end of the document.

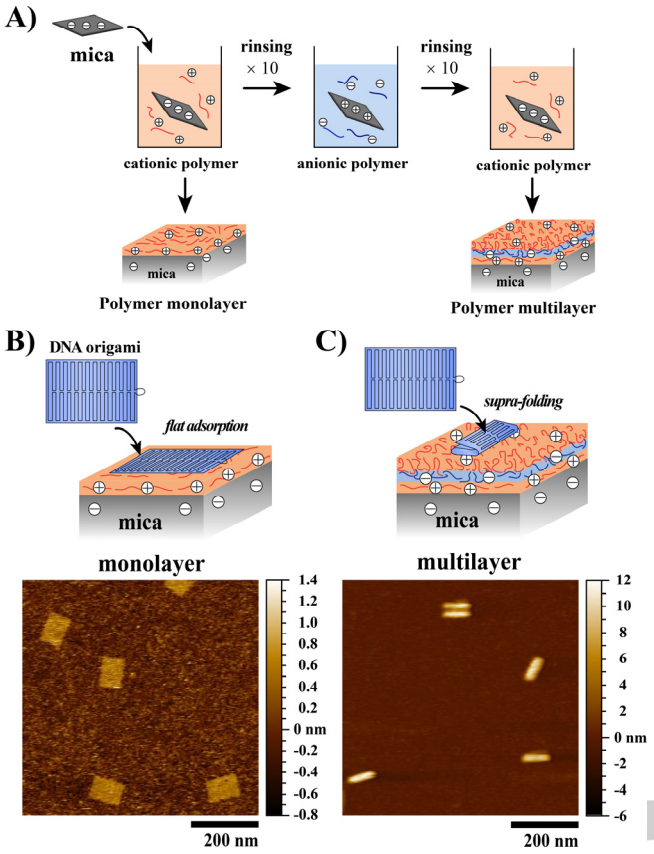

Figure 1. Schematic illustration of our experiment and main results. A) We used as a substrate a mica plate coated by either a polycationic monolayer (left) or a multilayered structure prepared by the layer-by-layer (LbL) assembly of an anionic polyelectrolyte layer sandwiched between two cationic polyelectrolyte monolayers (right). Surfaces were thoroughly rinsed after each polyelectrolyte adsorption step and before origami adsorption. B-C) Atomic force microscopy (AFM) images in liquid of tall-rectangle DNA origamis adsorbed on a cationic monolayer (B) or on a LbL multilayer with poly-L-lysine (PLL, M_W = 1000 - 5000) as the cationic polymer and tall-rectangle staples as the anionic polymer (C).

Figure 1 depicts our experimental system and demonstrates the main phenomenological results. Positively charged layers were created on negatively charged mica plates either by single layer adsorption of a cationic polyelectrolyte, or by sequential Layer-by-Layer (LbL) adsorption[28] of cationic and anionic polyelectrolytes (**Fig. 1A**). These polyelectrolyte-coated surfaces were then put in contact with a solution of tall-rectangle DNA origamis, prior to rinsing by buffer and direct imaging by Atomic Force Microscopy (AFM) in liquid. **Figures 1B and 1C** show AFM images of DNA origamis adsorbed on a monolayer of poly-L-Lysine (PLL) (*M*w = 1000 – 5000 g·mol^{-1}) and on a multilayer consisting of one layer of anionic polyelectrolyte (first arbitrarily chosen to be tall-rectangle origami staples) between two monolayers of PLL (PLL-staples-PLL), respectively. DNA origamis adsorbed on the PLL monolayer maintained their original shapes (**Fig. 1B**), as is usually observed for DNA origami adsorption on mica substrate either via ions present in the bulk (e.g., Mg^{2+}[29]) or previously treated by small multivalent cations (e.g., spermine[30]). In contrast, most of the tall-rectangle origamis adsorbed on the LbL multilayer appeared supra-folded into mainly rod-like shapes with one-third the area of the original origami and around 3 times its original height (**Fig. 1C**).

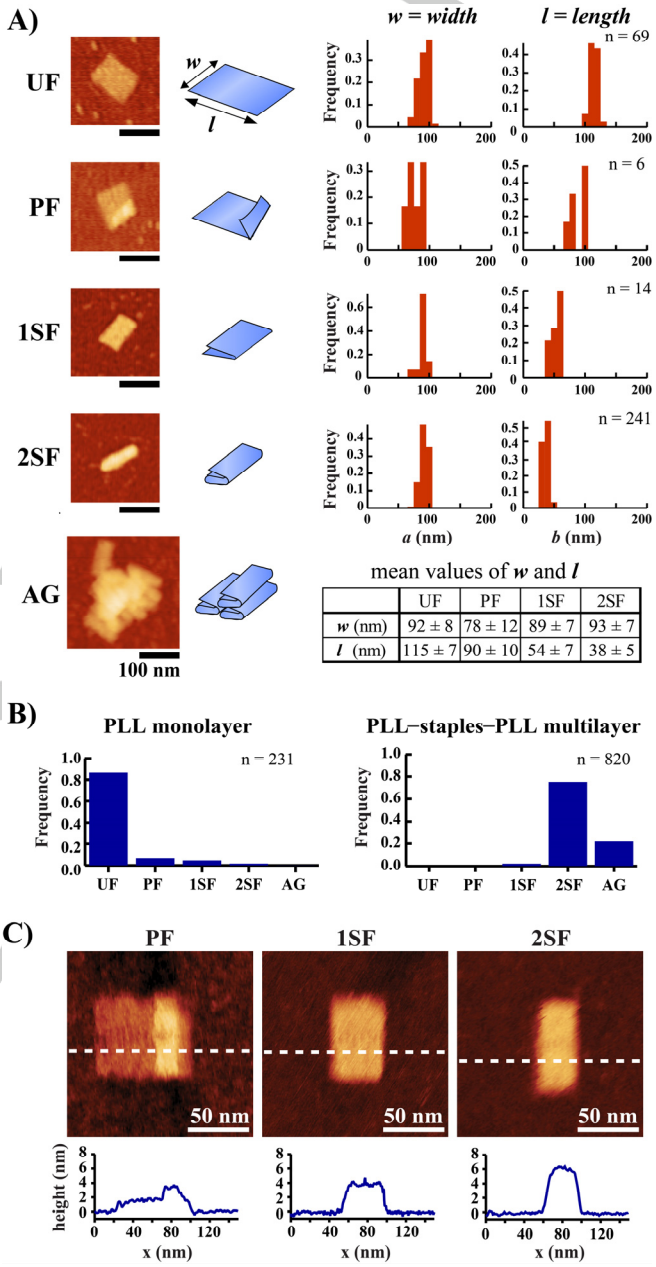

Figure 2. Categorization of the different objects observed after adsorption of tall rectangle origamis. A) Representative AFM images (in air) and indicative illustrations of the different types of adsorbed objects (left); Frequency of characteristic dimensions parallel (*"width" w*) and perpendicular (*"length" l*) to the DNA double-helix direction of each of these objects (right); Values (mean ± sd) of *w* and *l* for each category (right bottom). The category name refers to the degree of supra-folding: no (UF), partial (PF), one-time (1SF) or twice (2SF). AG denotes aggregates of supra-folded structures. B) Relative frequency of each category observed on a PLL monolayer (left) and a PLL-staples-PLL multilayer (right). C) High-resolution AFM images in liquid (top) and height profile analysis (bottom) of individual PF (left), 1SF (middle) and 2SF (right) supra-foldamers. In all figures, *n* gives the total number of analyzed adsorbed DNA origamis.

Other types of objects originating from tall-rectangle origamis were also observed on the LbL multilayers, which led us to categorize the adsorbed nanostructures into not supra-folded (UF: unfolded tall rectangles), three types of supra-foldamers (PF: partially supra-folded; 1SF: one-time supra-folded; 2SF: twice supra-folded), or aggregates of supra-folded structures (AG) (**Fig. 2A, left**). The aggregates were often composed of 2SF origamis arranged parallel to each other, indicating that supra-folded origamis were able to self-organize on the LbL cationic surfaces. The unfolded state, which constituted the majority (87%) of structures detected on monolayers, could not be detected anymore on multilayers where all objects were efficiently supra-folded and/or aggregated (**Fig. 2B**). Although the number of adsorbed objects increased with the adsorption time (t_{ads}), their distribution remained unchanged for $t_{ads} \geq 1$ min (**SI Fig. S1**), indicating that i) the supra-folding of DNA origamis occurred during or right after their adsorption on the multi-layered cationic surfaces and ii) it is a much faster process than conventional 3D origami assembly based on DNA base pairing.[8] Interestingly, the dimension parallel to the main double-helix direction in the initial tall rectangles (*"width" w*) stayed almost unchanged, whereas the perpendicular one (*"length" l*) underwent two- or three-fold decrease upon single or double supra-folding, respectively (**Fig. 2A, right**). These results show that supra-folding occurred parallel to the direction of double-stranded chains constructing the origamis, thus minimizing the bending of the DNA helices, a characteristic that was previously observed in programmed rolling behaviour.[15] This was confirmed by high-resolution AFM in liquid where the supra-folded parts were always found to be parallel to the double-stranded DNA direction that were distinguishable in the non-folded parts (**Fig. 2C, top left**). The supra-folding of tall-rectangle origamis was also accompanied by an increase of height from around 2 nm to 4 nm to 6 nm upon one-time and twice supra-folding respectively (**Fig. 2C, bottom**), showing that origamis supra-folded on themselves while maintaining their internal self-assembled structure.

To understand the role of the substrate properties on the supra-folding behavior, we systematically investigated DNA origami adsorption on various monolayer- or multilayer-treated mica surfaces prepared as in **Figs. 1-2** but with different kinds of cationic and anionic entities (**SI Figs. S2-S4, Tables S1-S2**). The polymeric nature of the layers was found to be determinant as using spermine, a short tetraamine, resulted in a large majority of DNA origamis adsorbing flatly without supra-folding in both monolayered (99%) and multilayered (97%) substrates. We conclude that, in that case, the cationic charges localized on the substrate offered poor accessibility for origami supra-folding to occur in 3D. In contrast, with cationic polyelectrolyte layers, the supra-folding yield was higher than with spermine, especially for long polyelectrolyte chains. This shows that polymeric connectivity between charges and conformational entropy in the adsorbed state (presence of loops), provided the substrate with more reconfigurability to electrostatically interact in 3D with the adsorbed origamis. Yet the supra-folding yield remained low with polymeric monolayers (**SI Fig. S4, Table S2**), probably because of their strong adsorption on the negatively charged mica substrate, leading to a high and rather flat cationic coverage (**Fig. 1B**). Interestingly, supra-folding was systematically and dramatically enhanced in the case of polyelectrolyte multilayers (**SI Fig. S2, Table S1**). It is known that LbL multilayer deposition leads to loopy, interpenetrated layers forming a so-called "fuzzy" nanostructure.[28] The resulting substrates thus appeared to be ideally soft and reconfigurable to interact with origamis in 3D and induce their supra-folding (**Fig. 1C**). Hence efficient supra-folding was observed with many kinds of LbL. This included 3-layered structures with a variety of cationic polyelectrolytes having different chemical natures (PLL, polyethyleneimine), chain lengths and internal structures (linear and branched), as well as 5-layered structures (PLL-staples-PLL-staples-PLL, **SI Fig. S5**). When we changed the intermediate anionic layer to sodium polystyrenesulfonate, supra-folding efficiency was low, a peculiar behaviour that might be due to a flatter conformation in the adsorbed state leading to a less loopy cationic surface. However, for all other tested anionic polyelectrolytes, such as double-stranded DNA of different sequences (salmon sperm DNA and lambda-phage DNA), efficient supra-folding was obtained (**SI Fig. S3, Table S1**), excluding a specific role of sequences and lengths of the nucleic acids used as intermediate layers. All these results demonstrate that supra-folding occurred upon origami adsorption when the substrate combined cationic surface charge with enough fuzziness to provide tridimensional reconfigurability and charge accessibility.

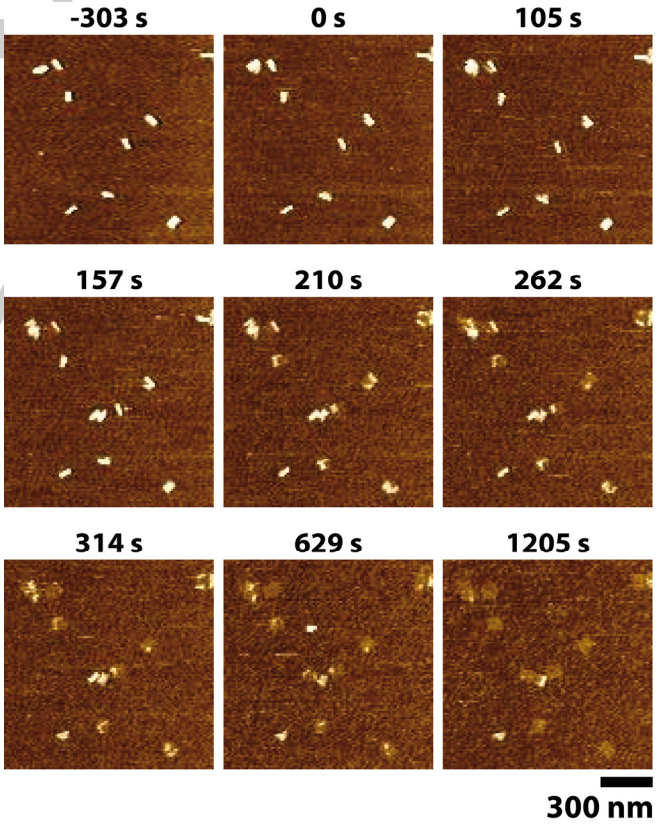

Figure 3. Heparin-induced unfolding of adsorbed origami supra-foldamers followed by live AFM imaging in liquid. Rectangle origamis adsorbed on a PLL-staples-PLL multilayer were imaged continuously using AFM in liquid. Heparin (9 µM in sulphate and carboxylate groups) was added at $t = 0$. Images are extracted from Movie S1.

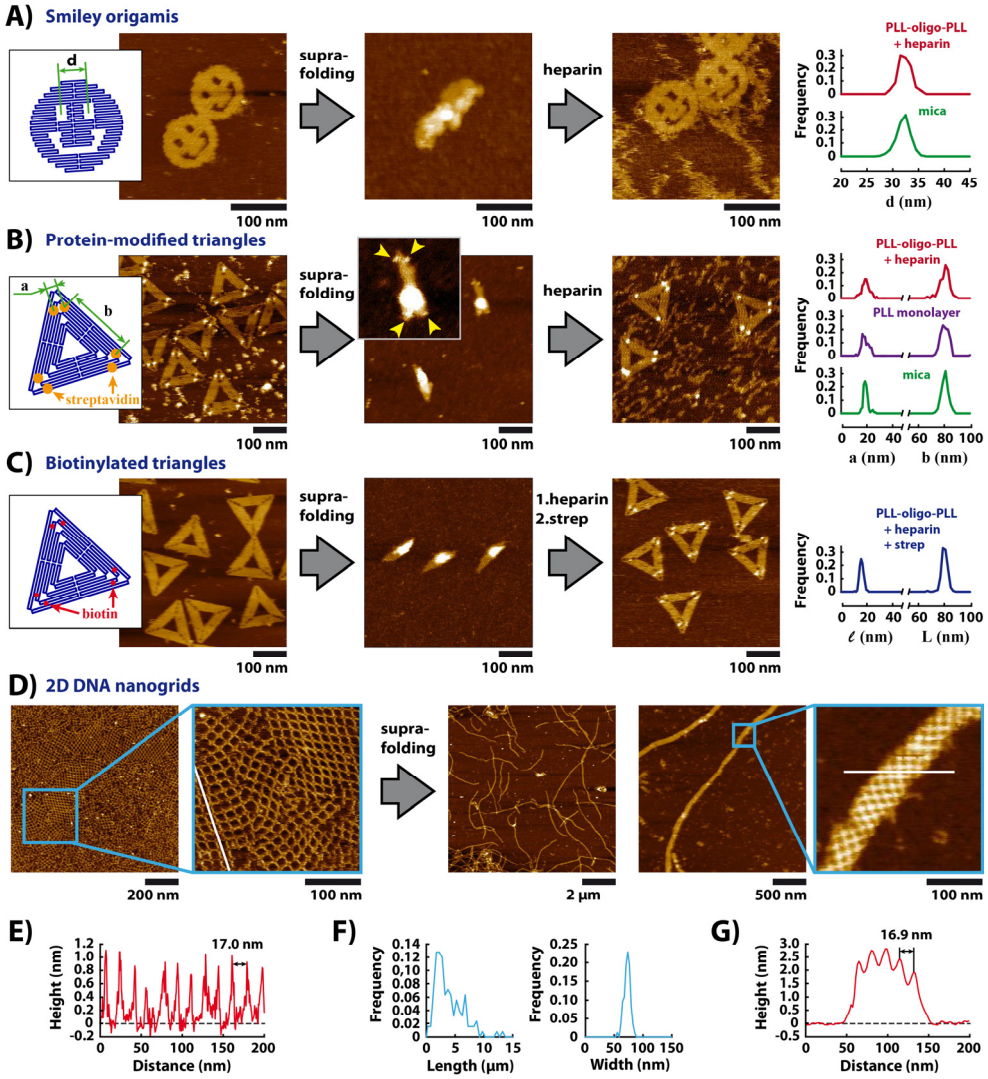

Figure 4. Supra-folding versatility demonstrated with various DNA nanostructures adsorbed on a PLL-staples-PLL multilayer. A-C) Smiley-shaped origamis (A), streptavidin-functionalized triangle-shaped origamis (B) and biotinylated triangle-shaped origamis (C) as observed by AFM in liquid before supra-folding (left, on mica), and after supra-folding on the multilayer before (middle) and after (right) addition of 15 µM heparin (A,B) or successive addition of 15 µM heparin and 2 µM streptavidin (C). Arrowheads in (B) indicate proteins in the supra-folded state. Graphics on the right display the distribution of characteristic lengths measured on a large number (*n*) of origamis: A) distance *d* between the smiley "eye" centers on mica (green) or after supra-folding and unfolding by heparin (red); B) distances between two tethered proteins in the same corner (*a*) or in the same edge (*b*) of origamis adsorbed on mica (green), on a PLL monolayer (purple) or on the PLL-staples-PLL multilayer after a sequence of supra-folding and heparin-induced unfolding (red); C) distances between tethered proteins (as defined in B) after supra-folding biotinylated triangles, unfolding by heparin and addition of streptavidin. D) AFM images in liquid of 2D DNA nanogrids before (left panels, on mica) and after supra-folding on the multilayer (right panels). E) Height profile in a nanogrid along the white line shown in D (second panel from the left). F) Size distribution of the length and width of the supra-folded ribbons observed in D. G) Height profile in a supra-folded ribbon along the white line shown in D (last panel on the right).

Since the supra-folding mechanism shared analogy with inter-polyelectrolyte complexation,[31] we explored the possibility of unfolding the supra-foldamers by adding a polyanion competitor, heparin, known to efficiently unfold electrostatically complexed linear DNA.[32,33] To this end, DNA origamis were first adsorbed on the PLL-staples-PLL multilayer, and we observed *in situ* their evolution over time by live AFM imaging in liquid at a fixed position (**Fig. 3, movies S1-S2**). The majority of origamis were found to be supra-folded on the substrate and did not evolve as long as the outer medium composition remained constant. In contrast, as soon as heparin was added to the medium, we observed a rapid evolution of the adsorbed supra-foldamers. In a few minutes, the height of each individual object decreased, accompanied by a planar extension perpendicular to the supra-folding direction. After 20 minutes of exposure, most of DNA structures adopted a stable shape reproducing the geometric features of the origami rectangles before their supra-folding. Successful unfolding was also observed by heparin addition to origamis initially surpa-folded on a LbL composed of 5 layers (**SI, Fig. S5**). Addition of heparin thus induced *in situ* unfolding of adsorbed supra-foldamers back to their original 2D shape and confirmed the interpolyelectrolyte complexation nature of the supra-folding mechanism.

Finally, we assessed the robustness of our actuation method for the structural 2D/3D reconfiguration of DNA assemblies with various structures, shapes, and functionality (**Fig. 4, SI Fig. S6**). First, similarly to tall-rectangles, origamis with other shapes, such as smiley- and triangle-shaped origamis, adsorbed flatly on the cationic monolayer but adopted supra-folded structures when adsorbed on the LbL multilayer and successfully unfolded back to their initial states upon exposure to heparin (**SI Fig. S7**). Fine structural details, even in complex shapes such as smileys were well preserved as shown by the identical mean eye-to-eye distance before (d = 32.0 ± 1.3 nm, n = 252) and after a sequence of supra-folding and heparin-induced unfolding (d = 32.3 ± 1.2 nm, n = 116) (**Fig. 4A, SI Table S3**). Similarly, protein-tethered origamis (**Fig. 4B left image**) adsorbed flatly on the PLL monolayer but supra-folded into 3D structures on the LbL substrate with a dramatic modification of the spatial protein distribution (**Fig. 4B middle image**, where detected proteins are pointed by arrowheads). Remarkably, heparin treatment led to unfolding of the protein-

functionalized origamis into their initial state (**Fig. 4B right image**), with a perfect recovery of the characteristic protein-protein distances (**Fig. 4B distributions** and **SI Table S3**). The same supra-folding → unfolding sequence was applied to biotinylated triangle-shaped origamis (**Fig. 4C**). Notably, further addition of streptavidin led to successful origami functionalization by the proteins (**Fig. 4C right image**) at the same positions (**Fig. 4C distributions** and **SI Table S3**) as in identical origamis but functionalized before supra-folding (**Fig. 4B** and **SI Table S3**). This shows that not only structural features but also functionality (here biotin reactivity) were preserved upon supra-folding and successive unfolding. The size of DNA origamis we studied was limited by the necessity of using a finite-size scaffold and, unless they oligomerized due to blunt end staking (e.g., in the case of smiley-shaped origamis) or occasionally aggregated, their supra-folding led to individual structures of limited dimension. To know whether 3D structures of higher dimension could be obtained, we characterized the supra-folding behaviour of so-called DNA nanogrids, which are scaffold-free and extended self-assembled structures composed by the repetition of a square motif of complementary oligonucleotides.[34] The motif size of the used nanogrid was 17 nm (**Figs. 4D left, 4E**). Remarkably, upon adsorption on the LbL multilayer, the nanogrids spontaneously supra-folded into well-defined 3D ribbons (**Fig. 4D, right**) with a width of around 75 nm, a length of a few micrometers (**Fig. 4F**) and a height between twice and three times larger than that of the initial 2D grid (**Fig. 4G**). The initial grid structure was preserved in the resulting ribbons, with a similar periodicity and square motif size (**Fig. 4G**). All these results show that supra-folding is a versatile method for the fast supra-folding of 2D DNA assemblies into 3D nanostructures that range from a compact size (DNA origami) to extended dimensions (nanogrids) and preserve both DNA structural features and site-specific functionality.

In summary, the present study revealed that 2D DNA nanostructures could undergo efficient and fast supra-folding on positive layer-by-layer polyelectrolyte substrates to give 3D supra-foldamers of nanometric (supra-folded origamis) to micrometric (ribbons) dimensions. We have brought evidence that it processed through an on-surface inter-polylectrolyte complexation mechanism. Orthogonal to DNA base-pairing, this actuation mechanism was proven efficient on various systems including DNA origamis of different shapes and functionality and DNA nanogrids, thus carrying a general character potentially applicable to many kinds of DNA-based nanostructures. Interestingly, this actuation principle was shown to be reversible as addition of heparin resulted in efficient switching of the supra-folded origamis back to their original 2D shape, in which structural features, reactivity and site-specific functionality were well preserved. Limited here to DNA-scaffolded streptavidin assemblies, we expect it to be applicable to the dynamically addressable DNA-scaffolding of various types of guests including functional proteins, active peptides, chemical groups or colloids. These results thus further emphasize some of the unique properties of fuzzy nano-assemblies produced by LbL as well as propose a simple yet novel and robust principle for the generic and reversible actuation of 2D/3D DNA-based nanostructures.

Acknowledgements

We thank M. Yokokawa (University of Tsukuba) for experimental support. This work was supported by the European Research Council (ERC) (European Community's Seventh Framework Programme (FP7/2007−2013)/ERC Grant Agreement No. 258782, D.B.), the French National Research Agency ANR contracts DYOR (ANR-18-CE06-0019, D.B.) and ActiveGEL (ANR-18-CE07-0001, S.R.), a Grant-in-Aid for JSPS Research Fellows (grant no. 15J04751, K. N.), and a JSPS Overseas Research Fellowships (K. N).

Keywords: DNA nanotechnology • Layer-by-layer • actuation • DNA origami • DNA nanogrid

[1] J. D. Watson, F. H. C. Crick, *Nature* **1953**, *171*, 737–738.
[2] L. Adleman, *Science* **1994**, *266*, 1021–1024.
[3] M. R. Jones, N. C. Seeman, C. A. Mirkin, *Science* **2015**, *347*, 1260901–1260901.
[4] W. B. Rogers, W. M. Shih, V. N. Manoharan, *Nat. Rev. Mater.* **2016**, *1*, 16008.
[5] F. Hong, F. Zhang, Y. Liu, H. Yan, *Chem. Rev.* **2017**, *117*, 12584–12640.
[6] P. W. K. Rothemund, *Nature* **2006**, *440*, 297–302.
[7] S. M. Douglas, A. H. Marblestone, S. Teerapittayanon, A. Vazquez, G. M. Church, W. M. Shih, *Nucleic Acids Res.* **2009**, *37*, 5001–5006.
[8] S. M. Douglas, H. Dietz, T. Liedl, B. Högberg, F. Graf, W. M. Shih, *Nature* **2009**, *459*, 414–418.
[9] D. Han, S. Pal, J. Nangreave, Z. Deng, Y. Liu, H. Yan, *Science* **2011**, *332*, 342–346.
[10] H. Jun, F. Zhang, T. Shepherd, S. Ratanalert, X. Qi, H. Yan, M. Bathe, *Sci. Adv.* **2019**, *5*, eaav0655.
[11] B. Saccà, C. M. Niemeyer, *Angew. Chemie - Int. Ed.* **2012**, *51*, 58–66.
[12] E. S. Andersen, M. Dong, M. M. Nielsen, K. Jahn, R. Subramani, W. Mamdouh, M. M. Golas, B. Sander, H. Stark, C. L. P. Oliveira, et al., *Nature* **2009**, *459*, 73–76.
[13] E. Benson, A. Mohammed, J. Gardell, S. Masich, E. Czeizler, P. Orponen, B. Högberg, *Nature* **2015**, *523*, 441–444.
[14] Y. Ke, L. L. Ong, W. M. Shih, P. Yin, *Science* **2012**, *338*, 1177–1183.
[15] H. Chen, T. W. Weng, M. M. Riccitelli, Y. Cui, J. Irudayaraj, J. H. Choi, *J. Am. Chem. Soc.* **2014**, *136*, 6995–7005.
[16] H. Ijäs, S. Nummelin, B. Shen, M. Kostiainen, V. Linko, *Int. J. Mol. Sci.* **2018**, *19*, 2114.
[17] J. K. Daljit Singh, M. T. Luu, A. Abbas, S. F. J. Wickham, *Biophys. Rev.* **2018**, *10*, 1283–1293.
[18] B. Yurke, A. J. Turberfield, A. P. Mills, F. C. Simmel, J. L. Neumann, *Nature* **2000**, *406*, 605–608.
[19] C. Kielar, S. Ramakrishnan, S. Fricke, G. Grundmeier, A. Keller, *ACS Appl. Mater. Interfaces* **2018**, *10*, 44844–44853.
[20] H. Chen, H. Zhang, J. Pan, T. G. Cha, S. Li, J. Andréasson, J. H.

Choi, *ACS Nano* **2016**, *10*, 4989–4996.
[21] Y. Sato, M. Endo, M. Morita, M. Takinoue, H. Sugiyama, S. Murata, S. M. Nomura, Y. Suzuki, *Adv. Mater. Interfaces* **2018**, *5*, 1800437.
[22] Y. Suzuki, M. Endo, H. Sugiyama, *Nat. Commun.* **2015**, *6*, 8052.
[23] M. W. Hudoba, Y. Luo, A. Zacharias, M. G. Poirier, C. E. Castro, *ACS Nano* **2017**, *11*, 6566–6573.
[24] S. Møller Sønderskov, L. Hyldgaard Klausen, S. Amland Skaanvik, X. Han, M. Dong, *ChemPhysChem* **2020**, *21*, 1474–1482.
[25] S. Julin, A. Korpi, Nonappa, B. Shen, V. Liljeström, O. Ikkala, A. Keller, V. Linko, M. A. Kostiainen, *Nanoscale* **2019**, *11*, 4546–4551.
[26] J. Mikkilä, A. P. Eskelinen, E. H. Niemelä, V. Linko, M. J. Frilander, P. Törmä, M. A. Kostiainen, *Nano Lett.* **2014**, *14*, 2196–2200.
[27] E. Kopperger, J. List, S. Madhira, F. Rothfischer, D. C. Lamb, F. C. Simmel, *Science* **2018**, *359*, 296–301.
[28] G. Decher, *Science* **1997**, *277*, 1232–1237.
[29] D. Pastré, O. Piétrement, S. Fusil, F. Landousy, J. Jeusset, M. O. David, L. Hamon, E. Le Cam, A. Zozime, *Biophys. J.* **2003**, *85*, 2507–2518.
[30] M. Tanigawa, T. Okada, *Anal. Chim. Acta* **1998**, *365*, 19–25.
[31] A. Estévez-Torres, D. Baigl, *Soft Matter* **2011**, *7*, 6746–6756.
[32] E. Ramsay, J. Hadgraft, J. Birchall, M. Gumbleton, *Int. J. Pharm.* **2000**, *210*, 97–107.
[33] S. Franceschi-Messant, N. Chouini-Lalanne, S. Rudiuk, I. Rico-Lattes, E. Perez, *Langmuir* **2008**, *24*, 8452–8457.
[34] H. Yan, S. H. Park, G. Finkelstein, J. H. Reif, T. H. LaBean, *Science* **2003**, *301*, 1882–1884.

Entry for the Table of Contents (Please choose one layout)

Layout 1:

COMMUNICATION

User-defined DNA nanostructures (origamis, nanogrids) undergo an astonishing higher-order folding transition, referred to as supra-folding, when they adsorb on soft cationic polymeric surfaces. Upon addition of a competitive anionic polyelectrolyte, supra-folded origamis unfold back to their original shape with preserved structural features and site-specific functionality (tethered function or protein).

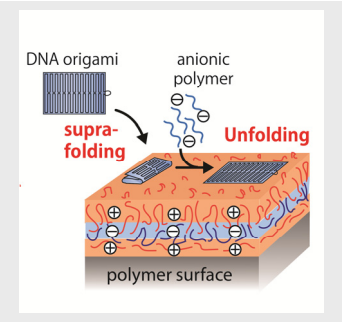

Koyomi Nakazawa, Farah El Fakih, Vincent Jallet, Caroline Rossi–Gendron, Marina Mariconti, Léa Chocron, Mafumi Hishida, Kazuya Saito, Mathieu Morel, Sergii Rudiuk, Damien Baigl**

Page No. – Page No.

Reversible supra-folding of user-programmed functional DNA nanostructures on fuzzy cationic substrates